Numerical Analysis of a 3-D Wing with an Active Flow Control Method

KNS Perera[1#], MM Basnayake[2], and SLMD Rangajeewa[3]

[1]*Kotelawala Defence University, Ratmalana, Sri Lanka*
[#] *<jamesnipun23@gmail.com>*

Abstract— *This research performs a numerical proof for enhancement of aerodynamic characteristic of a finite wing (Wing of Nanchang CJ-6 Aircraft) which is included with a conceptual design of an Active Flow Control (AFC) method. The active flow control design is a combination of continuous suction and blowing of air profile over the surface of wing. The effectiveness of active flow control model was tested by changing the number of slots and locations of suction and blowing. The numerical analysis was consisted with Reynolds-averaged Navier-Stokes (RANS) equations which were used in combination with a k-ω SST turbulence model.*

The optimum results were obtained for locating the blowing slots within the range of 0.3-0.47 in the chord length and suction slots within the range of 0.6-0.77 in the chord length. The Computational Fluid Dynamics (CFD) analysis was carried out at freestream conditions with a Mach number of 0.238, a Reynolds number of 6.166×10^6 and Angles of Attack from 0^0 to 15^0. The delaying of point of flow separation at higher Angle of Attack (AOA) was clearly observed and an increment of 30% and 24% in lift to drag ratio was obtained at an AOA of 0^0 and 12^0 respectively. The CFD simulations were performed using openFoam opensource software by giving the custom boundary conditions for the slot surfaces.

Keywords— **Active flow control, Aerodynamic characteristics, Flow separation**

I. INTRODUCTION

Active flow control method is a common flow control technique, that uses for the improvement of performances and manoeuvrability. Flow control includes preventing flow separation as well as delaying transition and both of which contribute to generate much higher lift to drag ratio(Donovan, Kral and Gary, 1998)(Kral, no date).

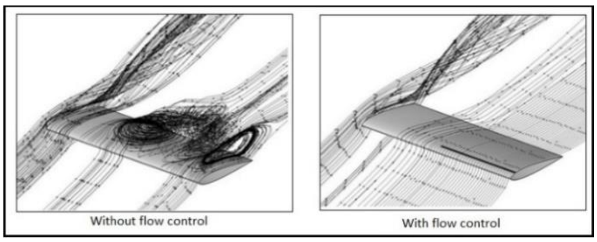

Figure 1-Effects of flow control(Zhang *et al.*, 2018).

There are variety of active flow control systems available. The following are the most prevalent active flow control models.

- Steady blowing- uses the extra air (or bleed air) from the propulsion unit (Rosenblum *et al.*, 2019).
- Co-flow jet arrays involving steady suction and blowing.
- Synthetic jet actuation- It is a zero net mass flux method (i.e. no separate mass of air is applied) and is a two-phase suction and injection procedure. (Rosenblum *et al.*, 2019).

This research focuses on applying of active flow control method on aerobatic aircraft. Continuous suction and blowing were incorporated as the active flow control method and its effects are elaborated in following chapters.

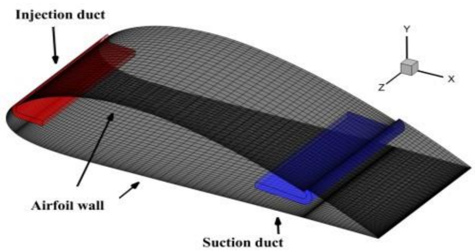

Figure 2 -Aerofoil with suction and blowing(Wang and Zha, 2019)

Nanchang CJ-6 aircraft which is used for aerobatic purposes at Sri Lanka Air Force has been selected for the research. These classical aerobatic aircrafts are lightweight and used to perform airshows. The wings of these planes are usually cambered and curved at the top and flat at the bottom of the wing. When considering aerobatics airframes designed for excessive aerobatics and 3D manoeuvres and having robust construction, it is indeed difficult for pilots to exercise direction while trying to execute high stress manoeuvres related to excessive thrust produced by the motors. So, it is necessary to avoid overloading the airframe (Aerobatics). When these aircraft expose to stall, the load acting on the control surfaces are greater and the effort that has to apply by the pilot on the control stick also greater. With active flow control methods, it is expected to delay the point of flow separation and to optimize the aerodynamic efficiency of the aircraft at lower as well as at higher AOA so that it improves the handling qualities of the aircraft.

II. METHODOLOGY AND EXPERIMENTAL DESIGN

The methodology comprises of three main sections.

A. *Designing and solid modelling of the wing*

The designing and solid modelling of the wing divides in to two main parts. First part is the solid modelling of the original wing of the Nanchang CJ-6 aircraft and second part is to design the wing including slots to apply suction and blowing with suitable locations.

The basic idea of applying both suction and blowing was generated after studying synthetic jet actuation. It is a two-phase suction and blowing method and in this research, it has converted it into a single phase flow control design. Further application of suction and blowing together, satisfy the Law of Continuity.

The solid modelling of the wing was done by using SOLIDWORKS 2018 software. The Geometric and characteristic data of the wing as per the manual are given in Table 1.

Table 1- Nanchang CJ-6 Wing specification.

Gross area (including area of the aileron)	$17m^2$
Wingspan (Theoretical value without wing tip light)	10.18m
Aspect ratio	6
Trapezoidal ratio	2
Sweepback angle (1/4 chord line)	0^0
Setting angle (Mid wing)	$2^0\ 30^/$
Chord length at the wing root	2.244m
Chord length at the wing tip	1.123m
Mean Aerodynamic chord length	1.747m
Dihedral Angle of the outer wing	7^0
Geometric angle of twist of the outer wing (Leading Edge downward)	3^0
Sectional Airfoil of the Wing root	NACA 23016
Sectional Airfoil of junction plane between the mid wing and the outer wing	NACA 23015.2
Sectional Airfoil of the wing tip	NACA 4412

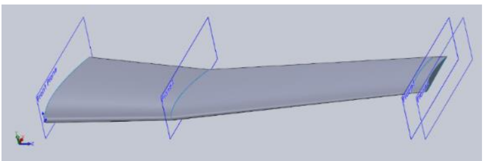

Figure 1- Solid wing model

Before designing the slots, it was necessary to consider the aileron data of the aircraft such as, the span and chord length. The aileron is occupied at the last quarter of the chord length of the wing, and it expands 1.91m along spanwise. Therefore, within the mentioned aileron span, the modifications to the wing can be done only up to 3/4 the chord length of the wing.

Since both suction and blowing was used as the active flow control method, the location and width of the slots were chosen by referring to the previous literatures.(Zha, Gao, *et al.*, 2006) (Wang and Zha, 2019). The specifications of slots in previous literatures were related to a wing made of NACA 6421 aerofoil and were matched to Nanchang CJ-6 wing model by calculating the mean location of flow separation and calculated by simulating the finite wing at an AOA of 4^0 (Zha, Paxton, *et al.*, 2006).

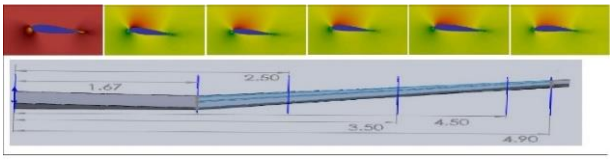

Figure 2- spanwise locations to obtain points of flow separation.

The location of flow separation at each spanwise location was identified by pressure variation along the surface and obtained locations are given in Table 2.

Table 2-locations flow separation

Spanwise location	**Location of flow separation**
0	0.75c
1.67	0.78c
2.5	0.78c
3.5	0.82c
4.5	0.85c
4.9	0.89c
5.01	No separation

The mean location of flow separation was calculated from above data, and it was about 0.81c which is similar to the previous research. Therefore, the slot locations and slots widths were directly taken and included into this research by converting the given locations and widths according to the dimensions and chord length of the Nanchang CJ-6 wing. Three wing models with slots were modelled with different active flow control designs by varying the number of slots and interchanging the location of suction and blowing. The details of each design are described below.

i. Design 1- One suction slot and two blowing slots (Blowing at trailing edge)

Table 3- Design-1 details

Type of the slot	**Chordwise location**	**Slot width**
Suction slot (S1)	0.34C	0.0046C
Blowing slot (B1)	0.61C	0.002C
Blowing slot (B2)	0.69C	0.002C

ii. Design 2- Two suction slots and three blowing slots (Blowing at trailing edge)

Table 4- Design-2 details

Type of the slot	**Chordwise location**	**Slot width**
Suction slot (S1)	0.34C	0.0046C
Suction slot (S2)	0.43C	0.0046C
Blowing slot (B1)	0.61C	0.002C
Blowing slot (B2)	0.69C	0.002C
Blowing slot (B3)	0.73C	0.002C

iii. Design 3- Three suction slots and two blowing slots (Suction at trailing edge)

Table 5- Design-3 details

Type of the slot	**Chordwise location**	**Slot width**
Blowing slot (B1)	0.34C	0.002C
Blowing slot (B2)	0.43C	0.002C
Suction slot (S1)	0.61C	0.0046C
Suction slot (S2)	0.69C	0.0046C
Suction slot (S3)	0.73C	0.0046C

The spanwise distribution of the AFC system is same in all the three designs. The AFC system is starts at the mid wing and ends at 0.19m behind to the wing tip. The following planform (Figure 5) describes the AFC system,

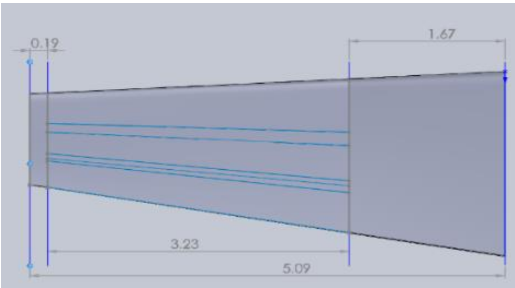

and all dimensions are given in meters.

Figure 3-Spanwise slot expansion

The mesh generation process divides in to two main sections. Before generation of the mesh with wing model geometry, first a domain mesh should be defined. Since this is a 3-D simulation, the domain dimensions should be compatible with the finite wing model. Therefore, the domain mesh dimensions were defined by referring to the previous literatures and considering the minimal free stream configurations.

The domain mesh included six patches and the wing model was placed on the patch which the type was given as **symmetricPlane** since the simulation is symmetric and only one wing is subjected for CFD simulation. Dimensions of the domain mesh are given in the Table 6.

Table 6- Domain mesh dimension

Direction (starting from the origin)	**Length**
+X	15c
-X	6c
+Y	6c
-Y	6c
+Z	10c
-Z	0

The mesh with wing model geometry was done with snappyHexMesh utility. The geometric features and other mesh specific features are included in the snappyHexMesh dictionary. Refinement regions were added to refine the mesh more precisely. After adding the refinement regions, the y-plus range can be able to bring less than 10, which must be satisfied to simulate with K-ω SST Model.

The surface features were derived from the original source file of surfaceFeatureExtract. SurfaceFeaturesDict is a sub dictionary where it contains the relevant extraction features.

The mesh with wing model geometry can be viewed as in Figure 6.

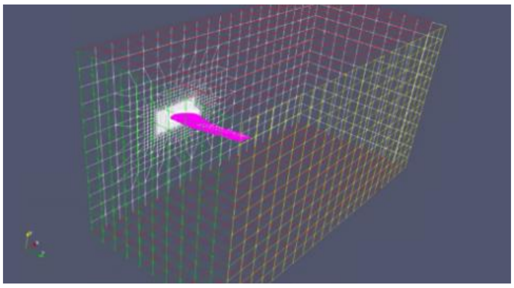

Figure 4-Final mesh with wing geometry

B. CFD Analysis

There are four maximum level flight speeds with respect to different altitudes possesses by Nanchang CJ-6 aircraft according to the aircraft flight manual. The mean maximum speed and atmospheric conditions at cruising altitude of 3000m was considered for the CFD analysis. The CFD analysis was performed by using openFoam 7 software.

C. Turbulence Model

Method of suction and blowing as an active flow control method basically takes place within the boundary layer. At higher angle of attack, the separation and wake area will be extended up to some considerable height into the free stream. Therefore, for solving of both flow near wall region and free stream, k-ω SST turbulent model was used. The turbulent parameters were calculated by 'Calculator for Estimation of Turbulence Properties Values', an online tool provided by Wolf Dynamics.

Table 7– Turbulence Parameters

Freestream Velocity	- U_∞	78	m/s
Turbulence kinetic energy	- κ	0.036504	m^2/s^2
Turbulence dissipation	- ε	4.875162	m^2/s^3
Specific turbulence dissipation	- ω	1483.902439	$1/s$
Turbulence Intensity	- T_U	0.2	%
Turbulence Length Scale	- T_{UL}	0.000128755	m
Kinematic Viscosity	- ν	2.14-e5	m^2/s
Eddy viscosity ratio	- $^{\mu_t}/_{\mu}$	0.8785714	

D. Boundary Conditions

All boundary conditions were set according to the mean maximum level speed and atmospheric conditions at altitude of 3000m of Nanchang CJ-6 aircraft.

Table 8- Initial Boundary conditions

Initial conditions		
Freestream Velocity	78	m/s
Pressure	7.01e4	Pa
Air density	0.90926	kg/m^3
Kinematic Viscosity	2.8-e05	m^2/s
Reynolds Number	6,165,900	

E. Custom Boundary Conditions for Application of AFC

In the solid modelling phase, the slot surfaces have already designed along with the wing. Therefore, it is not needed to re-identify an exact location to apply custom boundary conditions instead, custom boundary conditions can be applied to all cell faces in the slot surface patch.

The both angle and velocity for suction and blowing profiles, were decided according to the previous literatures(Zha, Gao, *et al.*, 2006). If the velocity is given as a magnitude ratio of velocity of ejection/ blowing to the free stream velocity (U_i/U_∞), for a suction patch, the velocity magnitude ratio is given as 0.9 and for blowing it was given as 1. In Design-1 and Design-2 the angle of suction profile was given as 90^0 and blowing profile was directed at an angle of 30^0.

In Design-3, suction profile was set as,

i. Suction slot (S1) – at an angle of 15^0
ii. Suction slot (S2) – at an angle of 45^0
iii. Suction slot (S3) – at an angle of 90^0

And blowing profiles were set at an angle of 30^0.

The code which describes the custom boundary conditions for a suction and blowing patches were programmed to activate suction and ejection of air profiles after completion of 0.001 seconds in the simulation.

The type of flow that considered here is incompressible turbulent flow. Therefore, solvers pisoFoam and pimpleFoam is suitable for these simulations. PimpleFoam was used as the solver for this research simulations as it is a large timestep solver and gives more accurate solutions as it is using two correctors. The simulation was carried out for 0.54 seconds and completed 58000 iterations and showed a convergency in solutions.

III. RESULTS

The non-dimensional coefficients resulted from each design are compared with the results of the original wing as a percentage of increments or decrements as per the equations given below. The sign of the percentage refers to the increment/decrement of the relevant non-dimensional coefficient compared to the original wing. The positive percentage defines an increment and negative percentage defines a decrement.

Lift gain/loss (%) =

$$\frac{C_L(Wing\ with\ AFC) - C_L(Original\ Wing)}{C_L(Wing\ with\ AFC)} \times 100\%$$

Drag Gain/Loss (%) =

$$\frac{C_D(Wing\ with\ AFC) - C_D(Original\ Wing)}{C_D(Wing\ with\ AFC)} \times 100\%$$

Aerodynamic Efficiency (L/D) Gain/Loss (%) =

$$\frac{\frac{L}{D}(Wing\ with\ AFC) - \frac{L}{D}(Original\ Wing)}{\frac{L}{D}(Wing\ with\ AFC)} \times 100\%$$

A. Design-1

The CFD analysis was restricted up to AOA of 6^0 due to the obtained results on lift and drag coefficients. The obtained results on lift and drag coefficients, lift to drag ratio and percentage increments in lift to drag ratio are included in the Table 9.

Table 9- Results obtained from Design 1

Solver - pimple Foam							
Suction velocity magnitude = 0.9							
Blowing velocity magnitude = 1							
	Original Wing			**AFC applied Wing**			**L/D comparison**
AOA	**C_L**	**C_D**	**L/D**	**C_L**	**C_D**	**L/D**	
0^0	0.19	0.016	12	0.18	0.013	13.62	11.8%
4^0	0.49	0.021	23.14	0.52	0.024	21.45	-7.8%
6^0	0.64	0.028	22.71	0.65	0.028	23.46	3.2%

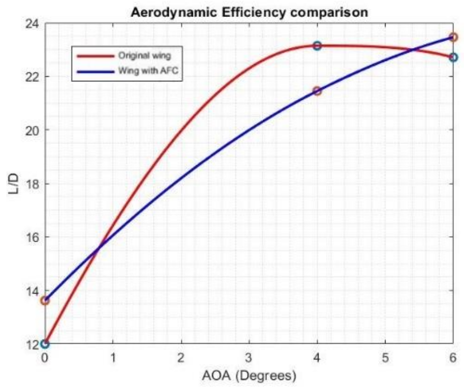

Figure 5- Aerodynamic Efficiency (L/D) comparison

B. Design-2

The CFD analysis was carried out for the AOA of 0^0, 4^0, 6^0, 9^0, 12^0 and 15^0 and the simulation was allowed to run up to 0.54 seconds. The velocity magnitude ratio for suction and blowing was kept as 0.9 and 1 respectively.

Table 10-Results obtained from Design 2

Solver - pimpleFoam						
Suction velocity magnitude (U_i/U_∞) = 0.9						
Blowing velocity magnitude (U_i/U_∞) = 1						
	Original Wing			**AFC applied Wing**		
AOA	**C_L**	**C_D**	**L/D**	**C_L**	**C_D**	**L/D**
0^0	0.192	0.016	12	0.195	0.0113	17.26
4^0	0.486	0.0206	23.03	0.525	0.0221	23.76
6^0	0.636	0.028	22.71	0.764	0.031	24.65
9^0	0.826	0.0482	17.14	0.829	0.047	17.64
12^0	0.637	0.117	5.444	0.645	0.09	7.167
15^0	0.526	0.166	3.169	0.558	0.171	3.263

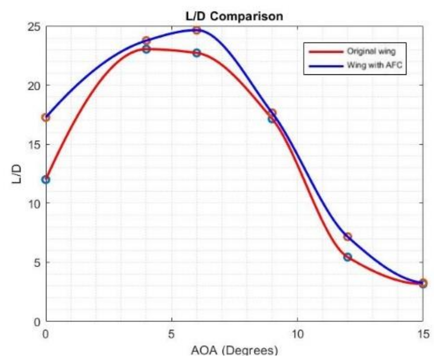

Figure 8-Aerodynamic efficiency comparison

C. Design-3

The lift to drag ratio of this design has a considerable increment at lower AOA as well as at higher AOA but in the middle range of AOA, the lift to drag ratio is not much greater than the lift to drag ratio of the original wing.

Table 11-Results obtained from Design 3

Solver – pimpleFoam						
Suction velocity magnitude (U_i/U_∞) = 0.9						
Blowing velocity magnitude (U_i/U_∞) = 1						
	Original Wing			**AFC applied Wing**		
AOA	**C_L**	**C_D**	**L/D**	**C_L**	**C_D**	**L/D**
0^0	0.192	0.016	12	0.269	0.0158	16.81
4^0	0.486	0.0206	23.03	0.506	0.0215	23.53
6^0	0.636	0.028	22.71	0.646	0.0284	22.75
9^0	0.826	0.0482	17.14	0.833	0.0442	18.85
12^0	0.637	0.117	5.444	0.815	0.101	8.069
15^0	0.526	0.166	3.169	0.658	0.164	4.012

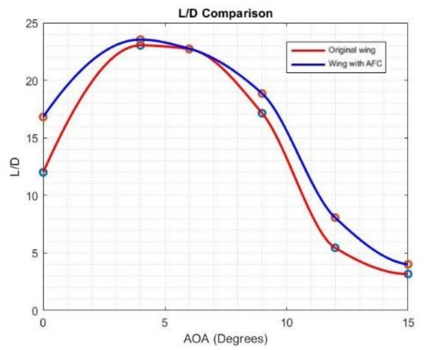

Figure 9-Aerodynamic efficiency comparison

IV. DISCUSSION AND CONCLUSION

The application of active flow control adds a disturbance to the flow. Therefore, each modification has to be done based on the requirement and considering the components such as primary controls of an aircraft. For the designing of active flow control model, required data was obtained from original manual of Nanchang CJ-6 aircraft.

The first design was a simple design followed by one suction slot and two blowing slots. The aerodynamic efficiencies obtained were not much greater compared to that of original wing. The lift has increased due to the flushing of the wake using the blowing of air from the blowing slots. But the contribution of the suction slot was not enough to slow down the air to counter the adverse pressure gradient.

Considering the facts of design-1, the design-2 was included with two suction slots and three blowing slots. The results were much better compared to that of design one. But at higher AOA, the results were not much greater. The reason was at higher AOA, the point of flow separation moves towards the leading edge (LE), so that blowing air profiles flushes only a part in the wake region. Effect of suction will become less efficient due to the varying momentum in the wake region which causes wake turbulence.

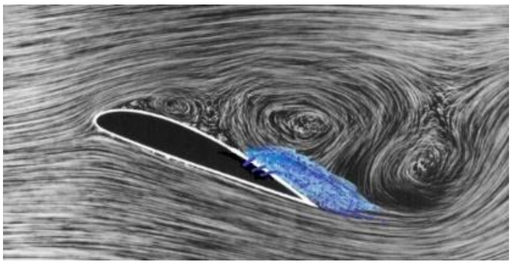

Figure 10-Blowing near trailing edge (TE)

Therefore in design-3, the blowing slots brought towards the LE and suction brought towards TE. Finally, Design-3 was included with two blowing slots and three suction slots. The blowing at LE retards the point of flow separation moving towards the leading edge at higher AOA and placing suction at TE accelerates the near boundary region in the wake and reduces the wake region by re-establishing the continuous flow. Therefore better results were obtained at higher AOA. Following table shows the comparion of aerodynamic charateristics with original wing.

Table 12-Lift, Drag and L/D comparison.

AOA	Lift comparison (%)	Drag comparison (%)	L/D comparison (%)
0^0	28.62	-1.266	28.62
4^0	3.953	4.186	2.132
6^0	1.548	1.408	0.142
9^0	0.84	-9.05	9.069
12^0	21.84	-15.84	32.53
15^0	20.06	-1.22	21.02

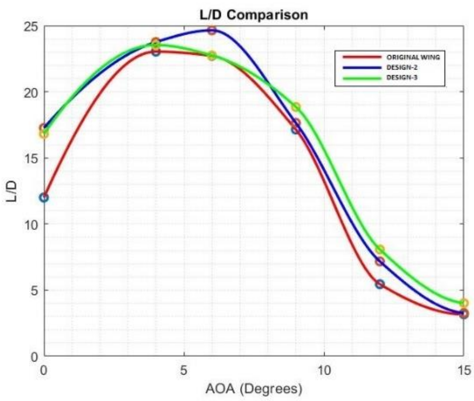

Figure 11 – Aerodynamic efficiency comparison of each design

The following figure shows a cross sections of wing taken from six span wise locations and taken from the simulation carried out at AOA of 12^0. The 2^{nd} row is where the AFC system is starting. Further, it is clear that the wake region is less in design 3 compared to design 2.

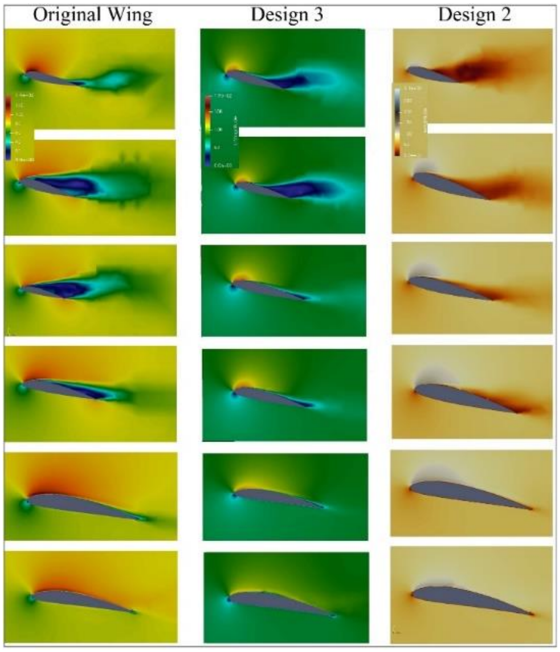

Figure 12 – Visual analysis of data from design-2 and design-3

The effect of active flow control methods on aerodynamic characteristics can be clearly identify by the above results. It was observed that the aerodynamic requirements of an aerobatic aircraft undergoing higher AOA and sudden AOA variations, can be satisfied by utilizing active flow control methods.

It is more concern on recovery of loss of lift during small and large angle of attack during Aerobatic manoeuvres. Greater Aerodynamic Efficiencies at middle range AOA is gives efficient fuel consumption and more economical but not much important in Aerobatic aircraft since these are not operating for commercial transportation purposes. Therefore, out of the three designs, design-3 satisfied the most desired characteristics. That is greater L/D ratios at lower and at higher AOA as elaborated in Figure 11

The CFD analysis was done by using k-ω SST as the turbulence model to solve both free stream and near boundary flow to improve the accuracy of results. The CFD simulations was done by using openFoam software and all the graphs were plotted using MATLAB R2019a software.

V. FUTURE WORK

In this research, it was concerning only the behaviour of aerodynamic characteristics of the wing. The stress analysis of the modified wing will be carried out in future to analyse the stress pattern and behaviour of the wing structure for further application.

Further it is important to validate the CFD results by using a wind tunnel. Therefore, it is required to design a 3-D model with AFC similar to design-3 along with a setup to do the suction and blowing with required velocities.

REFERENCES

Donovan, J. F., Kral, L. D. and Gary, A. W. (1998) 'Active flow control applied to an airfoil', in *36th AIAA Aerospace Sciences Meeting and Exhibit*. American Institute of Aeronautics and Astronautics Inc, AIAA. doi: 10.2514/6.1998-210.

Kral, L. D. (no date) *ACTIVE FLOW CONTROL TECHNOLOGY*.

Rosenblum, J. P. *et al.* (2019) 'Active flow separation control at the outer wing', *CEAS Aeronautical Journal*. doi: 10.1007/s13272-019-00402-4.

Wang, Y. and Zha, G. (2019) 'Study of 3d co-flow jet wing induced drag and power consumption at cruise conditions', *AIAA Scitech 2019 Forum*, (January). doi: 10.2514/6.2019-0034.

Zha, G., Paxton, C. D., *et al.* (2006) 'Effect of Injection Slot Size on the Performance of Co fl ow Jet Airfoil', 43(4). doi: 10.2514/1.16999.

Zha, G., Gao, W., *et al.* (2006) 'Numerical Investigations of Co-Flow Jet Airfoil with and without Suction'.

Zhang, J. *et al.* (2018) 'Aircraft control surfaces using co-flow jet active flow control airfoil', in *2018 Applied Aerodynamics Conference*. American Institute of Aeronautics and Astronautics Inc, AIAA. doi: 10.2514/6.2018-3067.

AEROBATICS, P. (N.D.). *AIRFRAME LIMITATIONS.*

ACKNOWLEDGMENT

We take this opportunity to express our profound gratitude to Mr. SLMD Rangajeeva sir, for the supervision and guidance, because of his sheer dedication to us throughout the research. We would also like to extend our gratitude to our Head of Department and all the senior lecturers and lecturers of the Department of Aeronautical Engineering at General Sir John Kotelawala Defense university.